J. Cell. Mol. Med. Vol 13, No 10, 2009 pp. 4219-4228

Abnormal connexin43 in arrhythmogenic right ventricular cardiomyopathy caused by plakophilin-2 mutations

Lee M. Fidler [a], Gregory J. Wilson [b], Fanfan Liu [a], Xuezhi Cui [a], Stephen W. Scherer [c], Glenn P. Taylor [b], Robert M. Hamilton[a, *]

[a] Heart Centre-Cardiology Division, The Hospital for Sick Children, Toronto, ON, Canada
[b] Paediatric Laboratory Medicine, The Hospital for Sick Children, Toronto, ON, Canada
[c] The Centre for Applied Genomics and Program in Genetics and Genomic Biology, The Hospital for Sick Children, Toronto, ON, Canada

Received: February 28, 2008; Accepted: July 15, 2008

Abstract

Arrhythmogenic right ventricular cardiomyopathy (ARVC) is a disorder of cardiomyocyte intercalated disk proteins causing sudden death. Heterozygous mutations of the desmosomal protein plakophilin-2 (PKP-2) are the commonest genetic cause of ARVC. Abnormal gap junction connexin43 expression has been reported in autosomal dominant forms of ARVC (Naxos and Carvajal disease) caused by homozygous mutations of desmosomal plakoglobin and desmoplakin. In tissue culture, suppression of PKP-2 results in decreased expression of connexin43. We sought to characterize the expression and localization of connexin43 in patients with ARVC secondary to heterozygous PKP-2 mutations. Complete PKP-2 gene sequencing of 27 ARVC patients was utilized to identify mutant genotypes. Endomyocardial biopsies of identified carriers were then assessed by immunofluorescence to visualize intercalated disk proteins. N-cadherin was targeted to highlight intercalated disks, followed by counterstaining for PKP-2 or connexin43 using confocal double immunofluorescence microscopy. Immunofluorescence was quantified using an Adobe® Photoshop protocol, and colocalization coefficients were determined. PKP-2 siRNA experiments were performed in mouse cardiomyocyte (HL1) cell culture with Western blot analysis to assess connexin43 expression following PKP-2 suppression. Missense and frameshift mutations of the PKP-2 gene were found in four patients with biopsy material available for analysis. Immunofluorescent studies showed PKP-2 localization to the intercalated disk despite mutations, but associated with decreased connexin43 expression and abnormal colocalization. PKP-2 siRNA in HL1 culture confirmed decreased connexin43 expression. Reduced connexin43 expression and localization to the intercalated disk occurs in heterozygous human PKP-2 mutations, potentially explaining the delayed conduction and propensity to develop arrhythmias seen in this disease.

Keywords: connexin43 • arrhythmogenic right ventricular cardiomyopathy • desmosome • gene mutation

Introduction

Arrhythmogenic right ventricular cardiomyopathy (ARVC) is a hereditary cardiomyopathy characterized by fibro-fatty replacement of myocardial tissue, ventricular tachycardia, syncope, and cardiac arrest [1]. ARVC affects between 0.02% and 0.1% of the population, and is a leading cause of sudden cardiac death in the third and fourth decade of life [2, 3]. Familial ARVC presentations have been mapped to 9 chromosomal loci, and identified gene mutations are predominantly those of cell-to-cell adhesion proteins, specifically, proteins comprising the desmosome [4, 5].

Desmosomes along with adherens junctions and gap junctions constitute the specialized organelles of the intercalated disk, the zone in which neighbouring ends of myocardial cells unite [6]. Each component of the intercalated disk upholds a unique role in cell function: adherens junctions stabilize cellular connections through interactions with the intracellular cytoskeleton; desmosomes facilitate connections between cells, transferring mechanical force within the myocardium; and gap junctions enable electrical impulse conduction from cell to cell, activating myocardial contraction [7, 8].

ARVC is associated with autosomal dominant mutations of desmosomal proteins, including plakophilin-2 (PKP-2), desmoplakin

*Correspondence to: Robert M. HAMILTON,
Heart Centre-Cardiology Division, The Hospital for Sick Children,
555 University Avenue, Toronto, Ontario M5G 1X8, Canada.
Tel.: +1-416-813-6142
Fax: +1-416-813-7547
E-mail: robert.hamilton@sickkids.ca

doi:10.1111/j.1582-4934.2008.00438.x

© 2008 The Authors
Journal compilation © 2009 Foundation for Cellular and Molecular Medicine/Blackwell Publishing Ltd

(DSP), junctional plakoglobin (JUP), desmoglein-2 (DSG-2) and desmocollin-2 (DSC-2) [9–11]. Two rare but severe autosomal recessive ARVC phenotypes with additional palmoplantar keratoderma and wooly hair, Naxos disease and Carvajal syndrome, are caused by homozygous mutations of JUP and DSP proteins respectively. Myocardial sections from victims of recessive Naxos disease and Carvajal disease have been studied using confocal immunofluorescence microscopy and demonstrate decreased gap junction connexin43 signal at the intercalated disks [12, 13]. Disruption of cell junctions associated with desmosomal protein abnormalities is believed to impair proper gap junction formation and function, leading to disturbances in cardiac electrical conduction and associated arrhythmias. Abnormalities of connexin43 expression at intercalated disks have been shown to occur in Boxer dogs with ARVC, although the specific gene mutation in this model remains unknown [14]. However, reduction in connexin43 expression has yet to be identified in humans with heterozygous desmosomal gene mutations causing ARVC [13, 14].

PKP-2, a member of the armadillo repeat domain family, improves cellular stability by bridging desmosomal cadherins and intermediate filaments of the cytoplasm [14, 15]. The development of cardiomyopathies as a result of autosomal dominant mutations of PKP-2 is consistent with the important structural function this protein exerts [16]. PKP-2 mutations underlying ARVC were initially identified by Gerul and colleagues in 32 (27%) of a series of 120 unrelated affected individuals [3]. Van Tintelen confirmed PKP-2 mutations in 24/56 (43%) individuals meeting ARVC Task Force criteria, making PKP-2 the most commonly mutated gene causing ARVC [17]. Despite the elucidation of desmosomal protein mutations as causes of this cardiomyopathy, little is understood regarding their role in cardiac arrhythmias.

We sought to examine the link between PKP-2 mutations underlying ARVC and the resulting arrhythmia, which occur in this disease. We hypothesized that mutations of PKP-2 would lead to reduced expression and/or localization of connexin43 at intercalated disks. A reduction in connexin43 gap junctions as a result of heterozygous mutations in PKP-2 may explain the ventricular conduction delay seen in patients with autosomal dominant ARVC and further develop our understanding of disease pathogenesis.

Materials and methods

Clinical characteristics of ARVC patients

Patients presenting to our cardiac arrhythmia program with any of non-sustained monomorphic ventricular tachycardia with LBBB morphology, a family history of ARVC or an epsilon wave underwent non-invasive testing included ECG, signal-averaged ECG, 24-hr ambulatory ECG, exercise testing, echocardiogram and magnetic resonance imaging. Those patients with one or more additional positive non-invasive findings underwent an electrophysiology study, right ventricular angiography and endomyocardial biopsy from the RV septum. Patients were approached for research (PKP-2, DSP, DSG) or clinical (PKP-2) genetic testing. Four patients with both a positive genetic diagnosis of a PKP-2 mutation and available residual tissue from endomyocardial study form the basis of this report.

Genetic analysis

Genetic analysis of PKP-2 in the four described patients was performed at two separate institutes. Two patients were sequenced at the DNA Diagnostics Lab at John Hopkins University, Baltimore, while two were determined by The Centre for Applied Genomics at the Hospital for Sick Children in Toronto. For DNA sequencing, polymerase chain reaction (PCR) amplification was performed, followed by genomic DNA sequencing. Twenty-seven patients with ARVC were screened for mutations in PKP-2 *via* DNA sequencing. PCR was completed using 20–50 ng of DNA in buffer [10mM Tris-HCl (pH 8.0), 50 mM KCl, 2.5 mM $MgCl_2$, 0.16 mg BSA, 0.01% gelatin], 0.4 mM dNTP's, 50 ng of each primer and 1 unit of Taq Polymerase (Applied Biosystems, Foster, CA, USA), resulting in total reaction mixtures of 25 μl. Reaction cycles were performed at 95°C for 2 min., 35 cycles at 94°C for 30 sec., 30 sec. of exon-specific temperatures, 72°C for 1 min., followed by 10 min. at 72°C, which correspond to the initial extension, denaturation, annealing, extension and final extension stages, respectively. Purification of DNA was performed using a CleanSeq (Agencourt Biosciences), followed by sequencing involving BigDye 3.1 chemistry on a 3730XL DNA Analyzer (Applied Biosystems, Foster, CA, USA). This study made use of human material and conformed to the principles outlined in the Declaration of Helsinki. Genetic research was performed with patient consent and approval of the Institutional Research Ethics Board.

Acquisition of tissues

Cardiac tissue was available for study from patients who had previously undergone endomyocardial biopsies as part of a clinical assessment for possible ARVC. Following clinical reporting of these specimens as analysed by light and electron microscopy, residual tissue was stored in liquid nitrogen. Institutional Research Ethics Board approval for immunofluorescence analysis of these residual samples was obtained. One to two sections per antibody were assessed by confocal immunofluorescence microscopy to characterize N-cadherin (an adherens junction protein with no known survivable mutations) as a marker of the intercalated disk, PKP-2 (the desmosomal protein of interest) and the ventricular gap junction protein connexin43. Control ventricular myocardial tissues for immunofluorescence analysis were obtained as frozen blocks from the native hearts of patients coming to heart transplantation for congenital heart disease without primary arrhythmia or myocardial failure (*e.g.* valvular disease) in which the myocardium, frozen immediately upon surgical removal of the native heart, was histologically normal.

Immunofluorescence and confocal microscopy

Seven-micrometer cryostat sections from patients and the controls were fixed with acetone at –20°C for 15 min. followed by air-drying for 30 min. The sections were rinsed in phosphate-buffered saline (PBS) and blocked in PBS with 2% normal donkey serum, 1% bovine serum albumin and 0.2% TritonX-100 for 1 hr at room temperature. Connexin43, PKP-2, DSP and N-cadherin antigens were examined following incubation with rabbit

© 2008 The Authors
Journal compilation © 2009 Foundation for Cellular and Molecular Medicine/Blackwell Publishing Ltd

anti-DSP (1:250, Serotec, Oxford, UK), mouse anti-PKP-2 (1:2, Progen Biotechnik, Heidelberg) and rabbit anti-connexin43 (1:200, Zymed Laboratories, San Francisco, CA, USA) antibodies for 1 hr. After rinsing with PBS, the sections were incubated with the corresponding secondary donkey antibodies (conjugated with Cy2 and Cy3, respectively) (Jackson ImmunoResearch, West Grove, PA, USA), diluted 1:200 and 1:500, for another 30 min. at room temperature. For double staining, sections were incubated with mouse anti-N-cadherin (1:500, Zymed Laboratories, San Francisco, CA, USA) or rabbit anti-pan cadherin (1:500, Sigma, St. Louis, MO, USA) and corresponding secondary antibody. Finally, DAPI staining was performed to identify nuclei. After a final rinsing step, sections were mounted with a 10% solution of polyvinyl alcohol containing 2.5% 1,4-diazabicyclo-2,2,2-octane (PVA/DABCO, both from Sigma, St. Louis, MO, USA), coverslipped, and visualized using a confocal laser scanning microscope LSM510 META (Carl Zeiss, Jena, Germany).

Quantitative localization and colocalization analysis

Double-stained images were obtained by sequential scanning for each channel to eliminate the crosstalk of chromophors and to ensure the reliable quantification of colocalization. Images for all four patients and two controls were acquired and processed for localization analysis of connexin43 to the intercalated disk. This analysis was performed using Adobe Photoshop on a Macintosh PC, adapting a previously published technique of luminescence analysis [18]. The outlines of intercalated disks were traced based on N-cadherin-stained samples, and the corresponding immunofluorescence signals for connexin43 and N-cadherin at the intercalated disk were sampled on a luminescence scale from 1 to 255. Approximately 5–10 intercalated disks were examined in roughly 5–10 different field images per sample. Sample background (non-intercalated disk) signal was subtracted and corrected connexin43 luminescence values representing the intercalated disks were expressed as a percentage of the corrected N-Cadherin luminescence $[(Cx43_{IC\ Disk}–Cx43_{Background})/N\text{-}Cad_{IC\ Disk}–N\text{-}Cad_{Background})*100\%]$. These percentages were then averaged and expressed as a final percentage luminescence in comparison to N-Cadherin for each patient.

Quantitative colocalization analysis of antigens was performed using Volocity Improvision 3.7.0 (http://www.improvision.com) for patients 2–4 and a single control. Background was corrected to remove the necessary number of pixels at all channels. Pearson's correlation coefficient (PCC), one of the standard measures of pattern recognition, was employed for colocalization of connexin43 and N-Cadherin.

Transfection of HL-1 mouse myocyte cells with PKP-2 siRNA

In parallel to examining endomyocardial biopsies from ARVC patients, HL-1 atrial myocytes were chosen for *in vitro* analysis. HL-1 cells have the ability to be continuously passaged and recurrently used in ARVC research [19–21]. These cells maintain the electrophysiological functioning of healthy cardiomyocytes and express near natural levels of connexin43, making them ideal for this particular research [21]. Ventricular myocytes, although anatomically appropriate for understanding ARVC pathogenesis, would be difficult to use in siRNA experimentation due to their limited lifespan.

The sense strands of the commercial hairpin siRNA (GenePharma, Shanghai, China) were homologous to a 19-nucleotide region in the PKP2 mRNA starting at nucleotide 192. The sequence of the siRNA for targeting and negative control siRNA were 5′-GGAUCCAGGAGCAGGUGCAdtdt-3′ and 5′-UGUCCGAACGUGUCACGUTTdtdt-3′ (sense sequence only). siRNA molecules with initial nucleotide hybridization at nucleotides 2121 and 2343 were also employed during the siRNA efficiency screening process. HL-1 myocyte cells were grown in Claycomb medium (JRH Biosciences, Lenexa, KS, USA) supplemented with 10% foetal bovine serum (JRH Biosciences), 0.1 M norepinephrine (Sigma, Saint Louis, MO, USA), 2 mM L-glutamine (Invitrogen, South San Francisco, CA, USA), and penicillin/streptomycin (10^4 U/ml P and 10^4 μg/ml S; Invitrogen, South San Francisco, CA, USA) in a humidified 5% CO_2-incubator at 37°C. HL-1 cells were plated at 8×10^4 cells/well in a 12-well plate and as monolayers on glass cover-slips at a density of approximately 2.5×10^4 cells/well in a 24-well plate. The next day, 0.5 μg siRNA was transfected into HL-1 cells using X-tremeGENE siRNA Transfection Reagent (Roche). The media was changed the following day and cells were experimented 96 hrs after transfection.

Immunoblot analysis

Cells in 12-well plates were rinsed twice with PBS, then added to 50 μl of RIPA lysis buffer (20 mM Tris-HCl, pH 8.0; 1% Nonidet P-40, 0.1%SDS, 0.5% sodium deoxycholate, and complete protease inhibitor; Roche), sonicated for 15 sec., and centrifuged at 12,000 rpm for 15 min. Protein concentration was determined using the Bradford protein assay (Bio-Rad Laboratories, Hercules, CA, USA). Aliquots of 10 μg of protein extracts were separated on SDS-polyacrylamide gels and transferred to nitrocellulose membranes. Membranes were blocked with 5% milk in Tris-buffered saline (TBS), then probed with a mouse anti-plakophilin-2 antibody (1:2 dilution, PROGEN Biotechnik, Heidelberg, German), mouse anti-N-Cadherin (1:400, Zymed Laboratories, San Francisco, CA, USA), or rabbit anti-connexin43 (1:200, Zymed Laboratories, San Francisco, CA, USA). The secondary antibody against mouse primary antibodies was goat anti-mouse IgG-HRP (1:10,000 dilution, Santa Cruz Biotechnology Inc.); against rabbit primary antibodies, a goat anti-rabbit IgG-HRP (1:5,000 dilution, Santa Cruz Biotechnology Inc., Santa Cruz, CA, USA) secondary antibody was used, followed by the detection of chemiluminescence.

Results

Clinical identification of ARVC

Of 27 patients with gene sequencing results for PKP-2, DSP and DSG, five PKP-2 mutations were identified. Residual endomyocardial biopsy tissue was available from four patients containing PKP-2 mutations. A clinical summary of patient characteristics, including major and minor task force criteria for ARVC diagnosis, as well as the identified genotypes are presented in Table 1. Two patients presented with syncope, and two with the sudden death of a young adult sibling, which were found at autopsy to have ARVC. Two patients had right ventricular global or segmental dilatation, and one had significant fibrosis on endomyocardial biopsy. Patients 2 through 4 showed signal-averaged ECG abnormalities, while patient 1 had sustained LBBB VT. However, only two patients fully met diagnosis by ARVC Task Force criteria, which are

© 2008 The Authors
Journal compilation © 2009 Foundation for Cellular and Molecular Medicine/Blackwell Publishing Ltd

Table 1 Summary of clinical ARVC manifestations in relation to patient genotype

Pt.	Age/Sex	Presentation	Wall Motion Abn.	Biopsy	ECG Depol. Abn.	ECG Repol. Abn.	Arrhythmia	F.H.	ARVC Maj.	Crit. Min.	Mutation
1	15/F	Syncope, VT	RV Dil.	69% fibrosis	–	T Inv.	LBBB VT	–	2	2	PKP-2: D460fsX464
2	11/F	Death of teenage brother: ARVC	–	5% fat (negative)	Abn. SAECG	–	–	+	1	1	PKP-2: L586fsX658
3	3/M	Syncope	RV Dil.	–	Epsilon, Abn. SAECG	–	–	–	1	1	PKP-2: R635W
4	17/M	Death of teenage sister: ARVC	RV Inf. Dyskin	–	Epsilon, Abn. SAECG	–	–	+	2	1	PKP-2: Q62K

Pt.,=patient; Abn.,=abnormality; Depol.,=depolarization; Repol.,=repolarization; F.H.,=family history; Crit.,=Criteria; Maj.,=major; Min.,=minor; F=female; M=male; VT=ventricular tachycardia; Inv.,=inversion; LBBB=left bundle branch block morphology; Dil.,=dilatation; Inf.,=infundibular; Dyskin.,=dyskinesia.

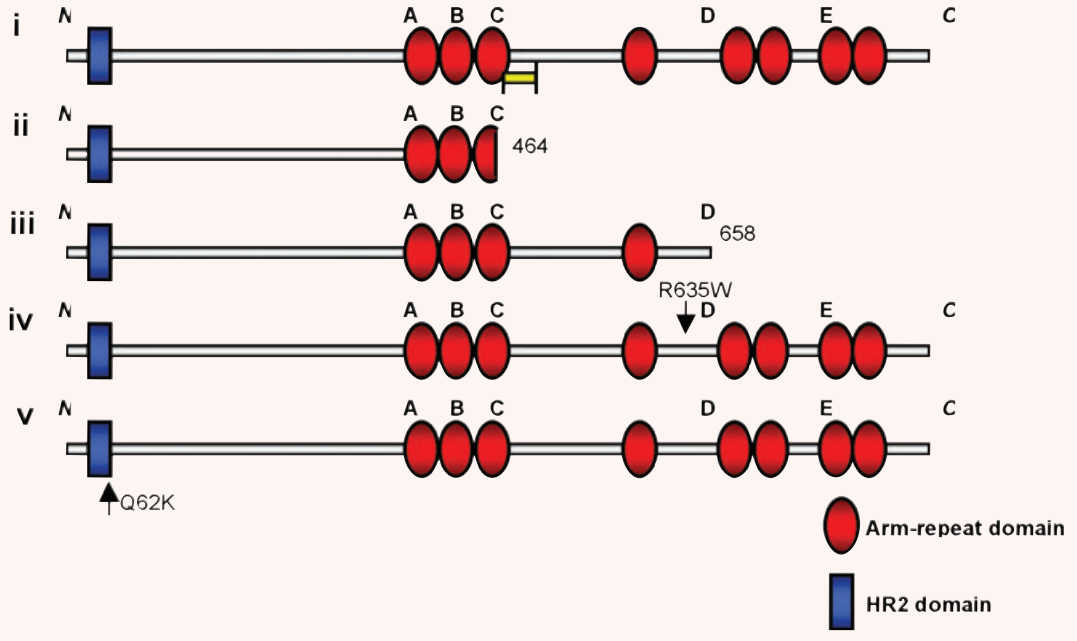

Fig. 1 Diagrammatic representation of the human PKP-2 protein. (i) Representation of the full length, wild-type form of PKP-2 showing its HR2 domain within the amino terminal head domain and 8 arm-repeat domains. Letters A–H represent each arm-repeat domain, which encompass amino acids 341-383, 385-424, 427-467, 571-616, 671-711, 719-758, 763-804 and 807-849, respectively. The amino terminal HR2 domain spans residues 29-60. Two isoforms of PKP-2 exist. The yellow bar beneath the C domain represents residues 460-503, which are absent in the PKP-2a configuration. Patients 1 through 4 are represented as ii, iii, iv and v, respectively. Arrows indicate the precise location of particular mutations, while carboxy terminal numbers indicate the length of the resulting protein in amino acids.

recognized to be only 50% sensitive for adults with ARVC and less sensitive for young patients.

Patient 1 was found to be heterozygous for a G to A transition at the upstream splice site border of intron 5 in the PKP-2 gene (Fig. 1.ii). This mutation disrupts the splice site consensus sequence, resulting in a truncated protein that is 464 residues in length (Fig. 1.ii). This mutation has not been previously reported in ARVC patients. Patient 2 showed an eight-nucleotide insertion

© 2008 The Authors
Journal compilation © 2009 Foundation for Cellular and Molecular Medicine/Blackwell Publishing Ltd

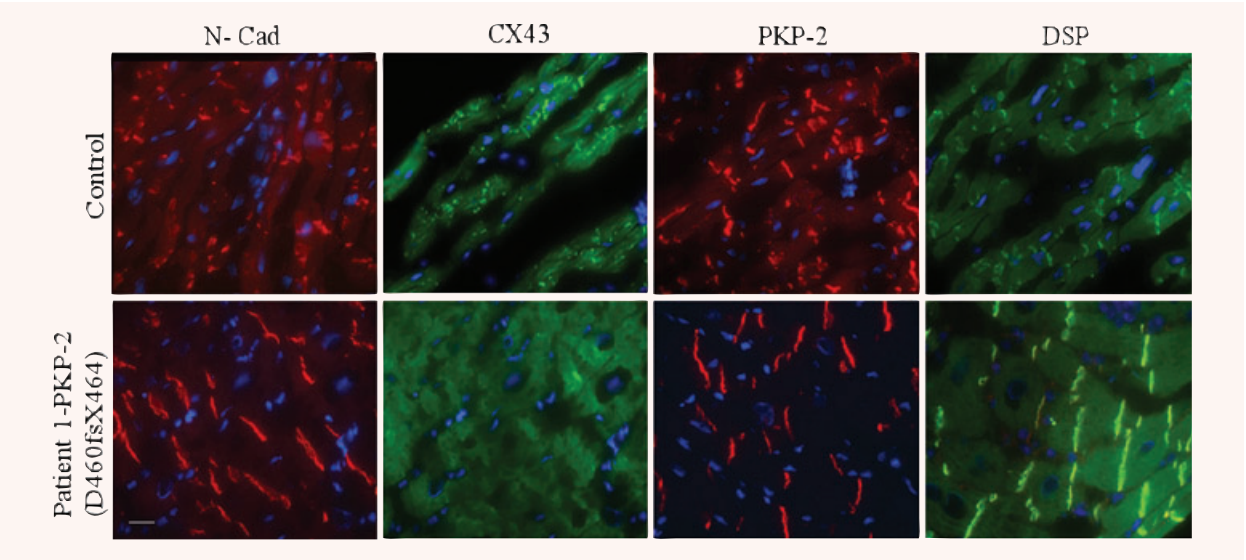

Fig. 2 Immunoflourescence studies staining with specific antibodies for N-cadherin, connexin43, PKP-2 and DSP in right ventricle tissue samples of Patient 1 and control. All tissue samples were stained using the same primary and secondary antibodies and were incubated for the same period of time. Blue signal represents cardiomyocyte cell nuclei, visualized with DAPI staining. The white bar corresponds to 10 μm.

(TTGACTCA) starting at nucleotide 1756 in the PKP-2 gene, which led to a prematurely truncated protein of 658 amino acids (Fig. 1.iii). This genotype has been previously described in ARVC pathogenesis [9]. A missense mutation, R635W, was elucidated in patient 3 (Fig. 1.iv). The underlying cause of this genotype is a C to T transition at nucleotide 1903. This novel mutation was not located in any recognized domains, but does target an evolutionarily conserved residue. Another previously recognized missense mutation, Q62K, caused by a C to A transversion at nucleotide 184, was discovered in Patient 4 to be the underlying cause of ARVC (Fig. 1.v) [22].

Connexin43 localization and expression is disrupted in plakophilin-2 mutant tissue

Immunofluorescent studies were used to visualize expression and localization of intercalated disk proteins in patients identified to have mutations of PKP-2. N-cadherin, connexin43 and PKP-2 proteins were visualized in both patients and controls. Patient 1 showed normal N-cadherin and PKP-2 positioning and expression, however, there was a noticeable decrease in connexin43 quantity (Fig. 2). While it was more difficult to visually discern decreased intercalated disk expression of connexin43 in the other three patients, increased ectopic expression of connexin43 was evident in patients 2–4 (Fig. 3). Patients 3 and 4 demonstrated abnormal connexin43 organization at the intercalated disk, where a punctate pattern of gap junction protein, rather than a continuous localization pattern was recognized (Fig. 3).

Abnormal connexin43 expression and colocalization to the intercalated disk were each quantified by assessing luminescence (Adobe Photoshop) and colocalization coefficients (Volocity), respectively. The percentage values of connexin43 luminescence in comparison to N-cadherin for patients 1–4 corresponded to values of 12.90%, 46.85%, 30.25% and 23.33%, respectively (Fig. 4). Thus, all patients showed decreased connexin43 luminescence in comparison to controls. Patient 1 showed a 48.46% reduction in connexin43 luminescence, while patients 2, 3 and 4 demonstrated reductions of 4.74%, 21.34% and 28.26% connexin43 luminescence with respect to control tissue (Fig. 4). Luminescence percentages for both controls 1 and 2 were calculated as 61.36% and 51.59% respectively (Fig. 4). Examining signal overlap of N-cadherin and connexin43 in merged images from patients 2–4 and a control sample allowed for the calculation of colocalization coefficients. These values are visually represented as yellow signal in Figure 5. The colocalization plot for the control patient showed a diagonal clustering pattern, representing a relatively high degree of protein overlap. The colocalization plots of patients 2, 3 and 4 were spread diffusely across the grid, indicating an increase in protein distribution and less colocalization. The control slide was determined to have a colocalization coefficient of 0.897. Patients 2, 3 and 4 showed progressively decreasing colocalization coefficients of 0.601, 0.445 and 0.125, respectively. Colocalization could not be performed for patient 1 because the image was not properly formatted for manipulation in the Volocity program, however, it can be inferred that connexin43 colocalization would be minimal, since connexin43 quantity was notably diminished.

© 2008 The Authors
Journal compilation © 2009 Foundation for Cellular and Molecular Medicine/Blackwell Publishing Ltd

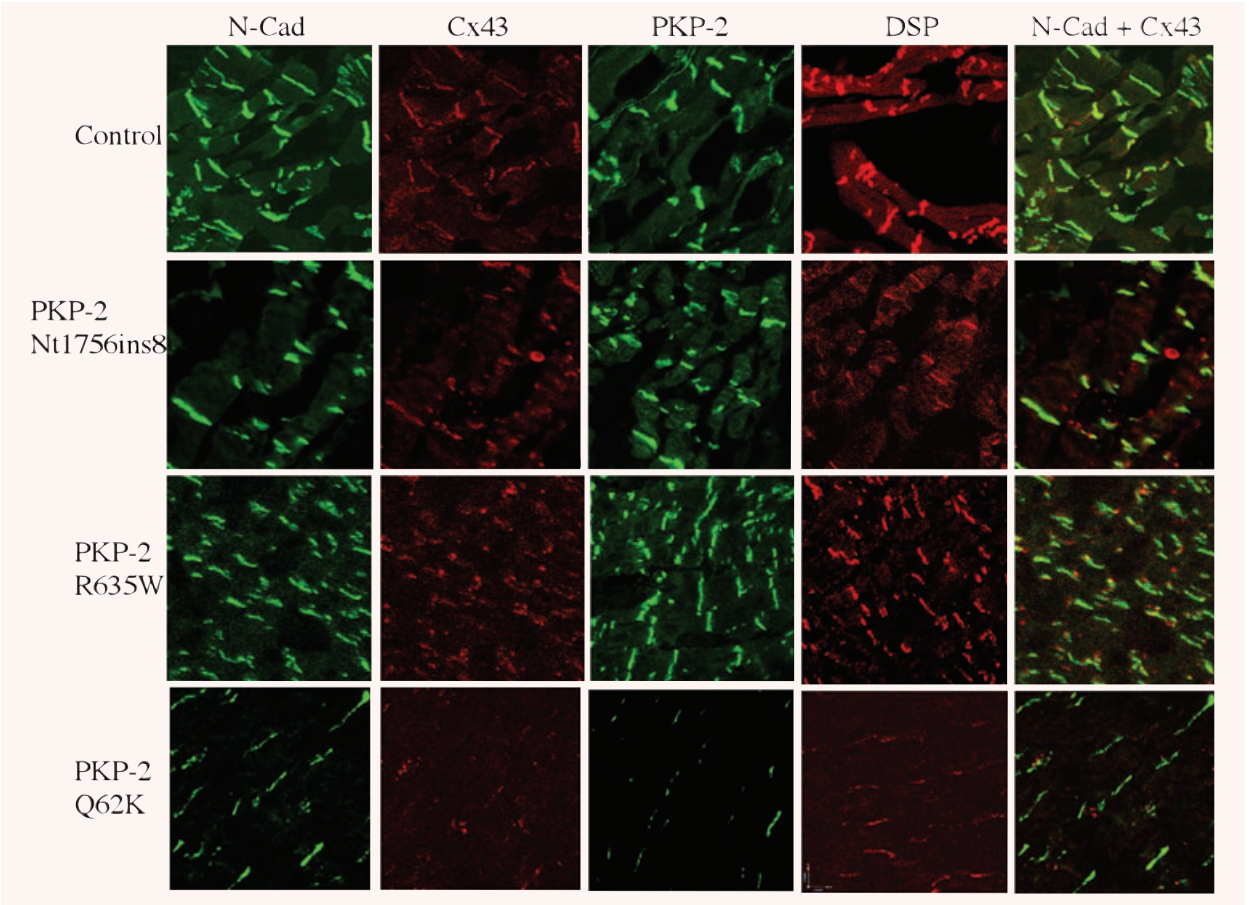

Fig. 3 Confocal images of patient tissue stained with immunofluorescent antibodies targeting both desmosomal and gap junction proteins. Three different patients and one control sample were examined using double labelling immunoflourescence experiments. Each patient sample demonstrated abnormal connexin43 expression as a result of a PKP-2 mutant genotype. The fifth column illustrates the overlap between connexin43 and N-cadherin, a marker of the intercalated disk. Abnormal localization and punctuate expression patterns were seen in all tissue samples except those from control patients. All tissue samples were stained using the same primary and secondary antibodies and were incubated for the same period of time. Photos were obtained using a LSM510 confocal microscope.

Plakophilin-2 siRNA alters connexin43 expression and localization in HL-1 cardiomyocyte cells

In support of our immunofluorescence results in ARVC diseased tissue, we examined the effect of PKP-2 suppression on gap junction protein expression in cell culture. To maximize PKP-2 mRNA silencing, several siRNA against the desmosomal protein were tested to identify the most efficient sequence. Three distinct siRNA sequences resulted in a similar reduction of PKP-2 protein expression. The degree of PKP-2 knockdown was determined by examining protein band density in transfected and non-transfected cells using Quantity One® software for a Macintosh PC. These results dictated which PKP-2 siRNA was to be used in examining the effects of desmosomal protein silencing on connexin43 expression. The absolute values for PKP-2 band density in control and siRNA transfected groups were 167052 and 49991, respectively, illustrating an over threefold decrease in protein expression. The amounts of GAPDH, as well as a PKP-2/GAPDH ratio for control and siRNA transfected cells, were determined to be 58572, 61199, 2.85 and 0.82, respectively. It was also determined by Western blot analysis that connexin43 expression did indeed decrease as a result of PKP-2 silencing, unlike the expression of a GAPDH control (Fig. 6A). Specifically, expression of non-phosphorylated connexin43 appeared to decrease more than phosphorylated protein, though both protein forms were reduced (Fig. 6A). Band density ratio to GAPDH was calculated for phosphorylated and non-phosphorylated connexin43 in non-transfected and transfected cells to be 0.62, 0.44, 0.52 and 0.28, respectively. To visualize the effects of PKP-2 siRNA on connexin43, immunofluorescent experiments were performed on transfected HL-1 myocytes.

© 2008 The Authors
Journal compilation © 2009 Foundation for Cellular and Molecular Medicine/Blackwell Publishing Ltd

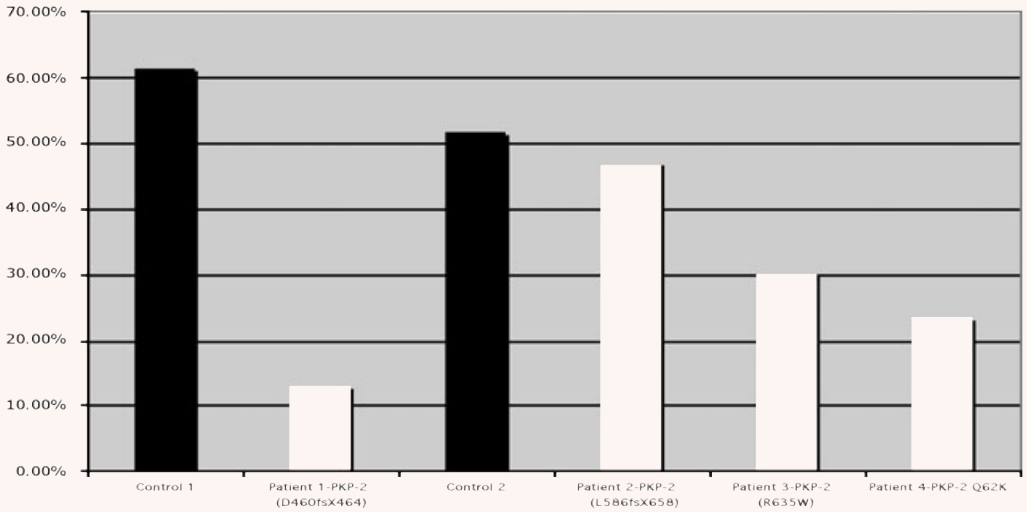

Fig. 4 Luminescence of connexin43 within the intercalated disc (minus background connexin43 luminescence) expressed as a percentage of N-cadherin luminescence (minus background N-cadherin luminescence). Patient tissue from four patients and two controls were examined to determine how plakophilin-2 mutations effect connexin43 luminescence at the intercalated disk. The determined percentages are a result of calculated sums of multiple pictures and intercalated disks.

Results of immunufluorescence experiments indicated that connexin43 undergoes dramatic reorganization following PKP-2 siRNA silencing. Four days after siRNA transfection, cells were exposed to PKP-2 and connexin43 primary antibodies, followed by incubation with targeted Cy2 and Cy3 tagged secondary antibodies respectively. Analysis of samples using fluorescence microscopy showed changes in both PKP-2 and connexin43. The amount of PKP-2 at the cell-cell borders was noticeably reduced in transfected cells (Fig. 6B). The residual PKP-2 protein tended to relocate to the perinuclear region, where it was found to colocalize with connexin43 (Fig. 6B). Rather than the even distribution of protein to cell junctions, a cytoplasmic clumping pattern was seen for PKP-2. Connexin43 also took on a punctuate expression pattern similar to that seen in PKP-2 mutated patients. Less gap junction protein was noticed at cell borders, mimicking the loss of connexin43 at the intercalated disks in ARVC patient tissue. Together with the results of patient tissue immunfluorescence, our results suggest that PKP-2 alterations have a deleterious effect on gap junction localization and expression.

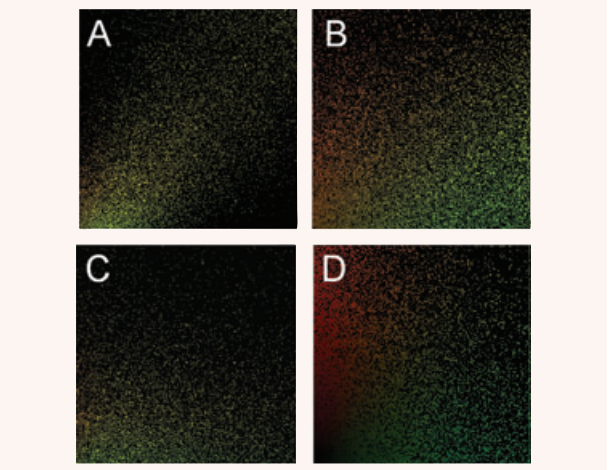

Fig. 5 Colocalization plots for connexin43 and N-cadherin from both ARVC patient and control tissues. The letters A, B, C and D correspond to the colocalization plots for Control patient, Patient 2, Patient 3 and Patient 4, respectively. Numerically, these plots correspond to values of 0.897, 0.601, 0.445 and 0.125. Calculations were made using the Velocity 3.0 program on a Macintosh PC. The above plots were calculated from the pictures shown in Fig. 3. Red signal indicates connexin43, green signal represents N-cadherin and yellow shows the overlap of the two.

Discussion

Our study demonstrates that gap junctions are remodelled in the myocardium of patients with autosomal dominant ARVC secondary to heterozygous PKP-2 mutations. This finding has only previously been demonstrated in autosomal recessive homozygous mutations of JUP and DSP underlying Naxos disease and Carvajal disease, respectively. However, unlike patients with Naxos and Carvajal disease, non-syndromal ARVC patients showed discernable differences in gap junction expression profiles between patients. Such variation can be attributed to the genetic diversity

© 2008 The Authors
Journal compilation © 2009 Foundation for Cellular and Molecular Medicine/Blackwell Publishing Ltd

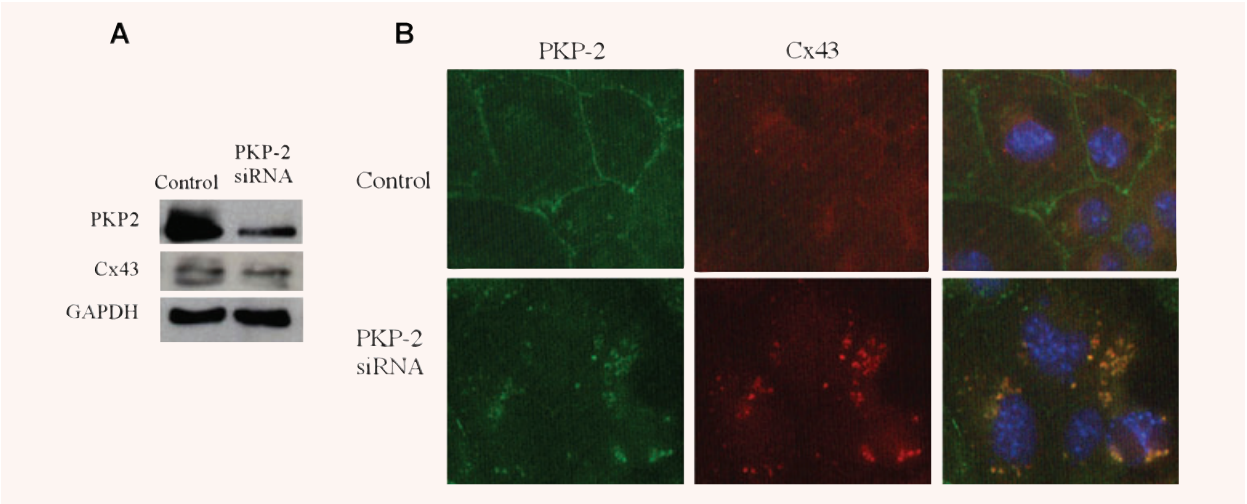

Fig. 6 Examining connexin43 expression and location in HL-1 cells following PKP-2 siRNA transfection. (**A**) Western blot analysis of PKP-2 and connexin43 expression compared to GAPDH following PKP-2 siRNA transfection. The top and bottom bands representing connexin43 illustrate phosphorylated and non-phosphorylated protein expression respectively. (**B**) Visualization of protein expression and localization in transfected and non-transfected cells using double labelling immunofluorescence. Nuclei were examined using DAPI staining. The third column represents the overlap of connexin43 and PKP-2.

in the patients examined. The decreased connexin43 expression and localization in all the examined ARVC patients implicates PKP-2 in connexin43 transcription, stabilization or transport.

Previous studies have been carried out to identify which portions of PKP-2 mediate interactions with certain protein-binding partners. The majority of PKP-2 interactions employ the amino terminal head domain, which has been identified to associate with DSG, DSC-2, β-catenin and α-catenin [15, 23]. Since the head domain is unaltered in the mutated form of protein for patients 1–3, we can hypothesize that many known protein interactions are maintained in these patients. However, loss of the arm-repeat domains in patients 1 and 2 may alter currently unrecognized binding events important for gap junction functioning. The low colocalization results seen in patient 4 may be due to the positioning of their mutation. The Q62K genotype of patient 4, located within the N-terminal head domain, is thought to be important in protein interactions, and when disrupted may directly lead to gap junction abnormalities through impairment of crucial binding events. The conversion of a glutamine to a lysine results in a slightly larger, positively charged residue, which due to its different properties may inhibit protein pairings. PKP-2 is now thought to be involved in the structural formation of both desmosomal plaques and adherence junctions (through head domain mediated interactions with α-catenin) broadening the mutational effects this protein may have on the structure of the intercalated disk [23].

Decreased connexin43 in ARVC patients may also be due to abnormalities in the nuclear functioning of PKP-2. PKP-2 is constitutively present in the nucleus and has previously been shown to bind to several transcription factors, including TFIIIB and RNA polymerase III [24]. Higher concentrations of PKP-2 have been found in the nucleus in the absence of the arm-repeat domains, suggesting that these domains may inhibit nuclear localization by either encoding nuclear export sequences or through alternative cytosolic protein connections [15]. The identified mutations in patients 1 and 2 result in truncated forms of PKP-2, which lack arm-repeat domains. An increase in truncated PKP-2 in the nucleus may alter transcriptional regulation, resulting in lowered gap junction expression. Our PKP-2 antibodies recognize a 24 amino acid carboxy-terminal sequence in the PKP-2 protein and therefore would not recognize patient 1 or 2 mutant PKP-2. The apparent normal levels of PKP-2 at the intercalated disk in all four patients may be explained by either transcriptional compensation or head domain mediated protein trafficking to the intercalated disk.

Although patient 3 had only a single amino acid substitution, their clinical ARVC presentation and changes in connexin43 expression were dramatic. The R635W mutation, though not in a domain region of PKP-2, replaces a positively charged arginine with a large non-polar tryptophan residue, and could have a major effect on protein function by disturbing ionic interactions and secondary protein structure. This particular arginine position is predicted to be located at a transition between helix and beta sheet structures (Swiss PDB viewer 3.7-Q99959). The arginine 635 is highly conserved across species, implying it serves a needed purpose.

Reorganization and altered expression of connexin43 was also seen in myocyte cell culture as a result of PKP-2 siRNA experiments. Oxford *et al.* similarly showed a decrease in connexin43 expression and redistribution of protein to the perinuclear region

© 2008 The Authors
Journal compilation © 2009 Foundation for Cellular and Molecular Medicine/Blackwell Publishing Ltd

following PKP-2 silencing [25]. As a result of reduced PKP-2 silencing, a global decrease in connexin43 was found, where both phosphorylated and non-phosphorylated protein states were decreased. Uncovering the reasons for the larger decrease in non-phosphorylated connexin43 will require more research, though it may be a result of increased degradation of cytoplasmic (non-phosphorylated gap junction) protein [26]. The redistribution of connexin43 to areas adjacent to cell nuclei in immunofluorescence results may also indicate removal of intercalated disk gap junctions and an increase in the cytoplasmic pool, possibly leading to enhanced protein destruction.

In order to directly link PKP-2 mutations to gap junction functioning our understanding of intercalated disk development must improve. A possible role of β-catenin in linking PKP-2 mutations to gap junction abnormalities has been proposed [25]. Further immunofluorescence experiments in myocyte culture examining β-catenin and α-catenin, which through ZO-1 has the capability of linking PKP-2 to connexin43, should be performed to clarify the role of adherence junction proteins in ARVC pathogenesis [27, 28].

The reduced localization of connexin43 to the intercalated disk likely affects gap junction functioning. The decrease of connexin43 among ARVC patients assessed in this study provides an explanation for the conduction delay and resultant arrhythmias seen in ARVC. Analogous results in myocyte cell culture using PKP-2 siRNA experiments further supports the notion of interaction between PKP-2 and gap junction proteins. Reduced gap junction protein expression in the intercalated disk was common to all PKP-2 mutations in our studies, as well as previously described homozygous JUP and DSP mutations in Naxos and Carvajal disease and the Boxer dog model of ARVC, representing a common mechanism for conduction delay and arrhythmias in this disease.

Gap junction remodelling in Naxos disease can be observed before structural abnormalities of fatty infiltration or fibrosis become apparent. Similarly, Patient 1 had minimal interstitial fibrosis or fatty infiltration on histomorphometric analysis. Our results demonstrate that in the presence of heterozygous PKP-2 mutations, normal amounts of PKP-2 appear to localize to the intercalated disk, but connexin43 gap junctions fail to colocalize there. Fibrofatty replacement of myocardium is likely a later phenomenon in the majority of patients with ARVC, representing a reaction to more complete mechanical dissociation as a result of desmosomal failure, or an additional molecular mechanism such as Wnt signalling [20].

ECG changes in ARVC implicate a major role for conduction delay, as may occur with reduced gap junction disease in the intercalated disk. Patient 3 showed epsilon waves, while Patients 1 and 2 were found to have late potentials on signal-averaged ECG, reflecting slow electrical conduction over the anterior right ventricle. Areas of slow conduction are one predisposing factor for re-entrant ventricular arrhythmias, which are seen in this disease and responsible in this patient group for sudden cardiac death.

The finding of reduced intercalated disk colocalization of connexin43 in association with PKP-2 mutations in ARVC suggests that PKP-2 is required to localize gap junction connexin43 protein to the cardiomyocyte intercalated disk. The PKP-2 mutations in our patients may result in decreased connexin43 colocalization, trafficking or transcription. Connexin43 expression and colocalization within the intercalated disk should be evaluated further in additional mutations of both these and other desmosomal proteins associated with ARVC. Examining connexin43 expression and colocalization within myocardial intercalated disks of ARVC patients might be a useful measure of disease expression, even in patients with as yet unidentified mutations.

Acknowledgements

We gratefully acknowledge Professor Ludwig Thierfelder for providing the plakophilin-2 primers for all 14 exons. This work was supported by the Caitlyn Elizabeth Morris fund of the Hospital for Sick Children Foundation and operating grant #NA6379 of the Heart and Stroke Foundation of Ontario.

References

1. **Thiene G, Nava A, Corrado D, *et al.*** Right ventricular cardiomyopathy and sudden death in young people. *N Engl J Med.* 1988; 318: 129–33.
2. **Frances RJ.** Arrhythmogenic right ventricular dysplasia/cardiomyopathy. A review and update. *Int J Cardiol.* 2006; 110: 279–87.
3. **Gerull B, Heuser A, Wichter T, *et al.*** Mutations in the desmosomal protein plakophilin-2 are common in arrhythmogenic right ventricular cardiomyopathy. *Nat Genet.* 2004; 36: 1162–4.
4. **Tabib A, Loire R, Chalabreysse L, *et al.*** Circumstances of death and gross and microscopic observations in a series of 200 cases of sudden death associated with arrhythmogenic right ventricular cardiomyopathy and/or dysplasia. *Circulation.* 2003; 108: 3000–5.
5. **Sen-Chowdhry S, Syrris P, McKenna WJ.** Genetics of right ventricular cardiomyopathy. *J Cardiovasc Electrophysiol.* 2005; 16: 927–35.
6. **Severs NJ.** Intercellular junctions and the cardiac intercalated disk. *Adv Myocardiol.* 1985; 5: 223–42.
7. **MacRae CA, Birchmeier W, Thierfelder L.** Arrythmogenic right ventricular cardiomyopathy: moving toward mechanism. *J Clin Invest.* 2006; 116: 1825–8.
8. **Borrmann CM, Grund C, Kuhn C, *et al.*** The area composita of adhering junctions connecting heart muscle cells of vertebrates. II. Colocalizations of desmosomal and fascia adhaerens molecules in the intercalated disk. *Eur J Cell Biol.* 2006; 85: 469–85.
9. **Syrris P, Ward D, Asimaki A, *et al.*** Clinical expression of plakophilin-2 mutations in familial arrhythmogenic right ventricular cardiomyopathy. *Circulation.* 2006; 113: 356–64.
10. **Pilichou K, Nava A, Basso C, *et al.*** Mutations in desmoglein-2 gene are associated with arrhythmogenic right ventricular cardiomyopathy. *Circulation.* 2006; 113: 1171–9.
11. **Heuser A, Plovie ER, Ellinor PT, *et al.*** Mutant desmocollin-2 causes

© 2008 The Authors
Journal compilation © 2009 Foundation for Cellular and Molecular Medicine/Blackwell Publishing Ltd

arrhythmogenic right ventricular cardiomyopathy. *Am J Hum Genet.* 2006; 79: 1081–8.

12. **Kaplan SR, Gard JJ, Protonotarios N, *et al.*** Remodeling of myocyte gap junctions in arrhythmogenic right ventricular cardiomyopathy due to a deletion in plakoglobin (Naxos disease). *Heart Rhythm.* 2004; 1: 3–11.
13. **Kaplan SR, Gard JJ, Carvajal-Huerta L, *et al.*** Structural and molecular pathology of the heart in Carvajal syndrome. *Cardiovasc Pathol.* 2004; 13: 26–32.
14. **Oxford EM**, **Everitt M**, **Coombs W**, ***et al.*** Molecular composition of the intercalated disc in a spontaneous canine animal model of arrhythmogenic right ventricular dysplasia/cardiomyopathy. *Heart Rhythm.* 2007; 4: 1196–205.
15. **Lapouge K, Fontao L, Champliaud MF, *et al.*** New insights into the molecular basis of desmoplakin- and desmin-related cardiomyopathies. *J Cell Sci.* 2006; 119: 4974–85.
16. **Chen X, Bonne S, Hatzfeld M, *et al.*** Protein binding and functional characterization of plakophilin 2. Evidence for its diverse roles in desmosomes and beta-catenin signaling. *J Biol Chem.* 2002; 277: 10512-22.
17. **van Tintelen JP, Entius MM, Bhuiyan ZA, *et al.*** Plakophilin-2 mutations are the major determinant of familial arrhythmogenic right ventricular dysplasia/cardiomyopathy. *Circulation.* 2006; 113: 1650–8.
18. **Kirkeby S, Thomsen CE.** Quantitative immunohistochemistry of fluorescence labelled probes using low-cost software. *J Immunol Methods.* 2005; 301: 102–13.
19. **Beffagna G, De Bortoli M, Nava A, *et al.*** Missense mutations in desmocollin-2 N-terminus, associated with arrhythmogenic right ventricular cardiomyopathy, affect intracellular localization of desmocollin-2 *in vitro*. *BMC Med Genet.* 2007; 8: 65.
20. **Garcia-Gras E, Lombardi R, Giocondo MJ, *et al.*** Suppression of canonical Wnt/beta-catenin signaling by nuclear plakoglobin recapitulates phenotype of arrhythmogenic right ventricular cardiomyopathy. *J Clin Invest.* 2006; 116: 2012–21.
21. **Claycomb WC, Lanson NA Jr, Stallworth BS, *et al.*** HL-1 cells: a cardiac muscle cell line that contracts and retains phenotypic characteristics of the adult cardiomyocyte. *Proc Natl Acad Sci USA.* 1998; 95: 2979–84.
22. **Lahtinen AM, Lehtonen A, Kaartinen M, *et al.*** Plakophilin-2 missense mutations in arrhythmogenic right ventricular cardiomyopathy. *Int J Cardiol.* 2008; 126: 92–100.
23. **Goossens S, Janssens B, Bonne S, *et al.*** A unique and specific interaction between alphaT-catenin and plakophilin-2 in the area composita, the mixed-type junctional structure of cardiac intercalated discs. *J Cell Sci.* 2007; 120: 2126–36.
24. **Mertens C, Hofmann I, Wang Z, *et al.*** Nuclear particles containing RNA polymerase III complexes associated with junctional plaque protein plakophilin 2. *Proc Natl Acad Sci USA.* 2001; 98: 7795–800.
25. **Oxford EM, Musa H, Maass K, *et al.*** Connexin43 remodeling caused by inhibition of plakophilin-2 expression in cardiac cells. *Circulation.* 2007; 101: 703–11.
26. **Sasano C, Honjo H, Takagishi Y, *et al.*** Internalization and dephosphorylation of connexin43 in hypertrophied right ventricles of rats with pulmonary hypertension. *Circ J.* 2007; 71: 382–9.
27. **Muller SL, Portwich M, Schmidt A, *et al.*** The tight junction protein occludin and the adherens junction protein alpha-catenin share a common interaction mechanism with ZO-1. *J Biol Chem.* 2005; 280: 3747–56.
28. **Girao H, Pereira P**. The proteasome regulates the interaction between Cx43 and ZO-1. *J Cell Biochem.* 2007; 102: 719–28.

© 2008 The Authors
Journal compilation © 2009 Foundation for Cellular and Molecular Medicine/Blackwell Publishing Ltd